

## Light Transmittance Ceramic Design-Computation with Robotics

Siyu Dong<sup>1</sup>, Jingjing Yan<sup>2</sup>, Shunyi Yang<sup>3</sup>, Xiangguo Cui<sup>4</sup>

University of Pennsylvania, Philadelphia, United States

<sup>1</sup> dongsiyu@upenn.edu;

<sup>2</sup> yanjj124@gmail.com

<sup>3</sup> vicnysy@upenn.edu

<sup>4</sup> xiangguo@upenn.edu

**Abstract.** Building envelope design incorporates a range of light-related analyses, often providing an essential feedback loop for shaping an envelope's performance, geometry, or components. This is true for solar radiation studies of envelopes, calculated irrespective of building material or assembly. Extending our light-related analysis to include diffuse lighting effects on a building interior presents an opportunity to explore the translucency, porosity, and forms of materials. Glazed architectural ceramic components fabricated using adaptive robotic manufacturing provide an opportunity to exploit material dynamics within the design and alleviate fabrication waste from molds, ultimately accelerating the production manufacturing system. In addition to analyzing the solar radiation on the building facade design, lighting effects can be engaged in profoundly different ways depending on the degree of design-production agency. The production process can be extended beyond automatic routines using robotic fabrication with levels of autonomous involvement that allow for alternative form expressions of the dynamic clay material. In addition to negotiating several design criteria, the design research will develop an aesthetic character originating from customized clay materials and robotic manufacturing processes for lighting transmittance architectural ceramics.

**Keywords:** Robotics Fabrication, Light Transmittance, Architectural Ceramics, Cellular Automata Algorithm, Material Malleability.

### 1 Introduction

Ceramics carries a wide range of transmittance and deformation potentials for robotics control with the research of its material property. We experiment with architectural clay, as the material of the product that is potentially translucent at a certain stage can respond to light. Studying the relationship between form, material properties, and porosity can help create different interior and exterior light effects and provide architectural product solutions for specific architectural functions. To ensure the ceramic product reach the expected transmittance level, research questions such as: what is the best clay material that can potentially carry the translucency characters? How to

control translucent effects in a ceramic screen? How to accurately map the translucent perforation to the overall form and the individual form of porcelain ceramic parts will be discussed with experiments from digital simulations to robot physical prototype manufacturing.

The research develops a system from design-computation to hardware toolkit through an experiment with the robotic approach to formative material processes. The lighting transmittance architectural ceramics will exhibit bespoke character that is integral to developing manufacturing and design-computation methodologies together, which also considers production effect and efficiency. Our objectives are to investigate the relationship between different clay bodies or ceramics' physio-material properties and their transmittance; to design the hardware toolkit in robotic fabrication to achieve precise lighting effect; to optimize the sufficient robot behaviors for different stages of deformation.

When operating various end effectors in robotics control, the deformation will be able to manipulate the amount of lighting that passes through. We can precisely manipulate the lighting effects by adjusting the robotics control behavior. The foam bead bedding system ensures the deformation to decrease clay thickness with typography variations to create the submarine reef's skin texture. Moreover, CA ruled perforation design with the perforating end effector provide openness for direct lighting passing through. The workflow investigates the light-transmitting effects of robotically perforated ceramic façade components. This paper presents one lighting transmittance design-to-fabrication system that engages with material research, hardware kit design, design-computation experiments.

## **2 Context**

Existing lighting-related design-research are mainly driven by digital solar radiation simulations tools. When Gutiérrez & Wanner (2016) proposed the design methodologies, they explored the materiality of clay by collaborating with renowned ceramicists and artists. Providing real-time optimization of form-finding is one aspect of testing the compatibility and interoperability of different software and design techniques. The full-scale ceramic products are fabricated by digital modelling and slip casting fabrication methodology. In his paper, he presents a production method developed along with construction and analytical data.

Clay material lighting transmittance was discussed in Ketchum's research article. Unlike what was previously assumed, translucency and thickness have an exponential relationship. In the presence of constant porcelain content, an increase in feldspar at the expense of flint results in a higher translucency. This research presents two directions to achieve clay material transmittance if one engages with physical clay deformation and composition. In Stylized Robotics clay sculpting (Ma et al.,2021), designers have developed traditional techniques for creating stylized cultural creations, such as the use of six-axis

robot arms to fabricate stylized cultures. Additionally, an algorithm was used to mimic brushstrokes of oil painting, allowing them to generate toolpaths for creating the styled cultures.

### 3 Robotic Training Methods

This paper shows the training process of the façade autonomous construction system. It includes the study of material transmittance, the study of robotic arm path behavior and transmittance, and tool fabrication.

#### 3.1 Material Transmittance

The experiment for identifying clay body lighting transmittance, including stoneware, earthenware, and porcelain, has been testified forehead.



Figure 1. Clay Body Transmittance Test

All samples are 3" x 3" square (Figure 1), and the thickness varies from 1mm to 5 mm. And all samples were placed in a dark room with the same brightness light source at the bottom and a light sensor at the top to capture the luminosity. The results showed that the samples numbered M3.0, M3.1, M3.2, M3.3, M3.4 showed luminosity effect.

Thickness (mm)	Tile to Lighting Source Distance (cm)				Color Variation
	0.5	0.8	1.1	1.5	
5mm					
4mm					
3mm					

Figure 2. Baked Porcelain Transparency Effect

Understanding that lighting could come from two perspectives: Material Transmittance property itself or creating porosity. The research started with playing with wet clay sheets. By manually manipulating the clay topography by carving, perforating, pressing, and semi-ring, the actions or behaviors can create more action marks on the surface and experience various lighting interfaces: angled lighting tunnels or straight poke holes. This study leaves many specific directions to explore (Figure 1). End effector, clay humidity, and robotics control behaviors can all impact the clay topography, the associated lighting effect, and the amount of lighting passing through.

Under the same quantities research method, another experiment among different baked porcelain samples revealed the desired lighting transmittance expectation. The intensity of transmittance and lighting color has a clear relationship between tiles' thickness, brightness, and the distance between the lighting source and tile surface: the further the distance is, the more separated and the looser the lighting effect. The thicker the tile is, the warmer the lighting color will be. (Figure 2)

### 3.2 Tooling study

This experiment explored that the light transmission of baked clay was negatively correlated with thickness. Although porcelain is opaque in its unbaked state, the ideal light transmission of clay after baking can still be achieved by finding a relationship between the depth of pressing and the thickness of the clay sheet.




Name	Times	Deformation Result	Force Analysis
Crater Bending System	5 times in each points		The overall force is not uniform, and fractures are likely to occur at the interface between the porcelain clay tile and the base.
Lollipop Bending System	5 times in each points		Overall, the force situation is good, the form is largely intact, and there are unevenly stressed interfaces in places with large deformation.
Rolling Bending System	5 times in each points		The overall force is good, but during the drying process, there are some problems with the shrinkage of the porcelain clay tiles, resulting in cracks at the junction of the clay tiles and the rolling.

Fig.3 Bedding result test and result

By using the same end effector and squeezing down it the same number of times, we tested the stresses on these three bedding systems, as well as the

richness of clay deformation. The final base was chosen based on its best stress and variation. (Figure 3)

During the late stage of the experiment, both the "Rolling bedding system" and "Crater Bedding system" produced severe cracks, which may be the result of water loss and shrinkage in the porcelain clay pieces limited by the base. Furthermore, both systems exhibit very homogeneous deformation, which makes it challenging to produce a façade with rich thickness variation. Therefore, we chose irregular spheres as the base. (Fig.4)



Fig.4 Final Choice—Transformable Foam Beans Bedding System

### 3.3 Robotic path and Transmittance

This experiment tested the correlation between the extrusion height and light transmission of the ABB 120 robotic arm when using the Transformable Foam Beans Bedding System. As well as the force limits of the porcelain clay under compression by the robot arm.

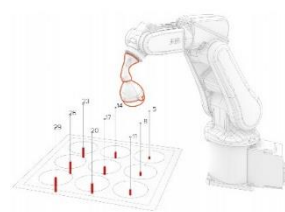


Fig.5 Progressive Pressing Robot Control Behavior

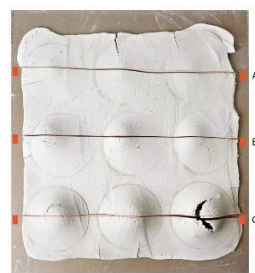


Fig.6 Plan View

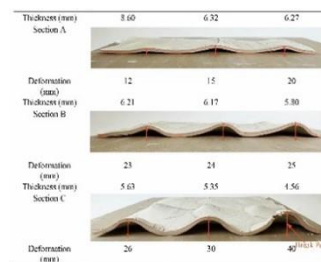


Fig.7 Relationship of Clay Deformation and Robot Pressing Times and Depth

The ABB 120 robotic arm pressed a ceramic sheet with a thickness of 10 mm (Figure 5), with the depth gradually increasing from 12 mm to 40 mm. As the pressing depth increased, the thickness of the ceramic piece decreased from 8.60 mm to 4.56 mm, and when the pressing depth reached 40 mm, the ceramic piece fractured, which indicates that this is the limit of the pressing depth. It shows that this is the limit of its pressing depth. (Figures 6,7)

## 4 Robotics Manufacturing System Workflow

The purpose of machine involvement in manufacturing decisions is to make the building façade part of the structural, aesthetic and modulating interior light environment and to provide designers with the opportunity to incorporate material behavior as a process driver into their design workflow. Use material behavior as a process driver in the design workflow. Once the system is trained and correlations between fabrication parameters and extruded sculpted geometry are established, it can switch back and forth between these two sets of data and the system can build a structurally sound, evenly lit façade based on the light requirements of the site.

The system uses the Penn Collection as an example to demonstrate the process of machine involvement in the fabrication of the façade system, including inputting the light requirements of the target space, translating the light requirements into the form of the façade, performing structural simulation of the façade, and making real-time decisions on the location and number of openings by the machine through sensors during the construction process. (Fig. 8).

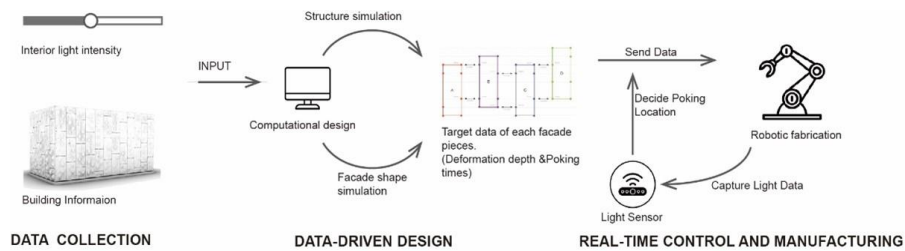


Fig.8 Robotic Manufacturing System Workflow

### 4.1 Global Structural Analysis Driven Pattern Generation

In the system of force analysis simulation of the facade, the combination of the extrusion experimental data and the facade generation system ensures the stability of the facade structure in the extrusion process and reduces the waste of porcelain clay. Using the mechanical analysis software Karamba 3D, the study first calculates the forces exerted on the panels of the façade, where wind load and self-weight are the main types of external forces, whereas the connection points between the panels and the main structure of the building and between the panels are the points of restraint. Based on the calculation results, red and blue areas correspond to strong tensile and compressive forces, while white represents uniform forces. Perforations will undermine the structural performance of the panel, so we opted to distribute the deformation mainly at locations where the panel is highly stressed (i.e., red, or blue areas) and distribute the perforations at locations where there are even stress distribution as white areas.

At a technical level, random points are first generated in the rectangular border of the panel, and then the color mesh generated by the Karama 3D force calculation is used to provide color data for each point in the same location. The program calculates the radius of the deformation circle of the points automatically based on the RGB value of the mesh vertex. A circle whose color is closest to blue or red has a larger radius, while vice versa, a circle whose color is further from blue or red has a smaller radius, as shown in Fig.9.

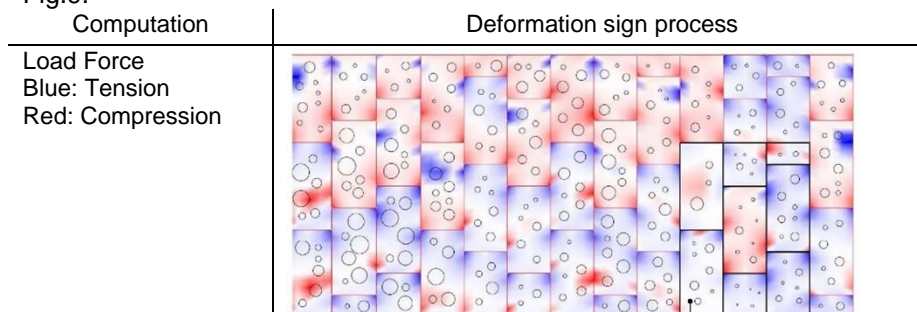


Fig.9 Relocation Circles According

## 4.2 Cellular Automata Algorithm for Perforation

The cellular Automata algorithm determines the angular distribution, orientation, and distribution of the hole. In python, each dot represents holes with a diameter of 5 mm. Each point is a class instance with information about the three types of holes we define, which are stored as an instance property called state. In each iteration, the type of the hole changes its type according to the number of types of its neighbours. If the current state is 0 and the number of holes with state 2 is less than a certain number, the state of the instance changes to 2. The three types of holes change cyclically and are finally distributed evenly on each panel. (Fig.10)

```
#Get sums of neighbor states
For i in range(len(neigh)):
    s = neigh[i].state
    if s==0: n0+=1
    if s==1: n1+=1
    if s==2: n2+=1
    n +=1
    total +=s
aver = total/n
if self.state == 0 and
n2<30: self.state =2
elif self.state == 1 and
n2<30: self.state =0
elif self.state == 2 and
n2<30: self.state =1
```

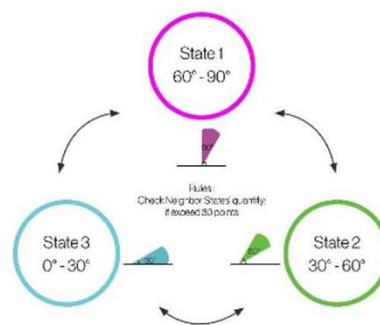


Fig.10 CA State for Perforated Angle



With a hypothesis program set up, an input usage with a gradient grayscale to represent different lighting requirements programs was generated. Different CA rules were applied to different regions of black, gray, and white, so that points located in different color regions were subjected to different scales of gravitational and repulsive forces from different neighbor types, thus affecting their behavior during motion and the final pattern formed, as shown in Figure 11.

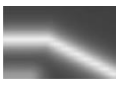
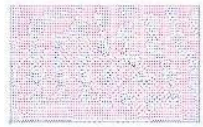
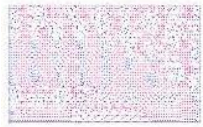





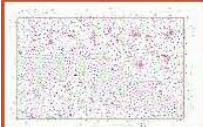
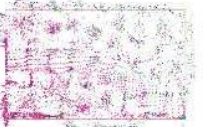
Input image	Time	CA Rules and input Grid					
 Black: more light  Grey: Mid-level light	1	Neighbor Range. Attr 1000 Repel300	Gray: 3* R 2* A	Neighbor Range. Attr 1000 Repel300	Gray: 3* R 2* A	Neighbor Range. Attr 1800 Repel1800	Gray: 6* R 8* A
		Black: 1* R 0* A	White: 3* R 0.6 A	Black: 6* R 2* A	White: 3* R 0* A	Black: 8* R 2* A	White: 1* R 0.6*A
							
White: Minimal light	2						
	3						

Fig.11 Lighting Transmittance Analysis for CA Rule

Take the first column as an example, for all points, the points within 1m from the point have gravitational force on the point, and the neighbors within 300 mm have repulsive force on it.

If the point is currently in the black area, the gravitational coefficient is 2 and the repulsive force is 1; if it is in the grey area, the gravitational coefficient is 2 and the repulsive force is 3; if it is in the white area, the gravitational coefficient is 0.6 and the repulsive force is 3. Images 1-3 in Fig.13 represent the calculation results of the distribution corresponding to different iterations and the orientation of the hole in the direction of the combined force of the surrounding neighbors on the point. The orientation of the hole in the direction of the joint force of the surrounding neighbors on the point.



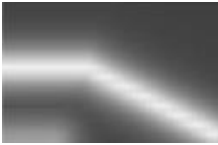
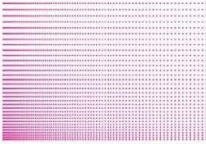
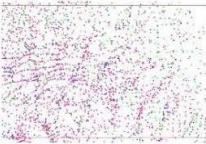
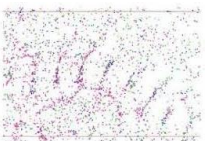


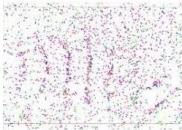
Input Image	CA Rules		
	Black Area	Gray Area	White Area:
	Force:		
	Repel	20	
	Attraction	2	8
	Vector:	2	4
	Repel	2	2
	Attraction	0	-1
		2	[0,0,0]
Input Grid	Iterations		
Uneven Grid	3	5	
			
Even Grid	3	5	
			

Fig.12 Perforation Grids and Iterations

In addition, we also try to add the influence of global variables to make the starting grid produce a gradient effect with different distances, as shown in Figure 15.

### 4.3 Data-driven Manufacturing Workflow

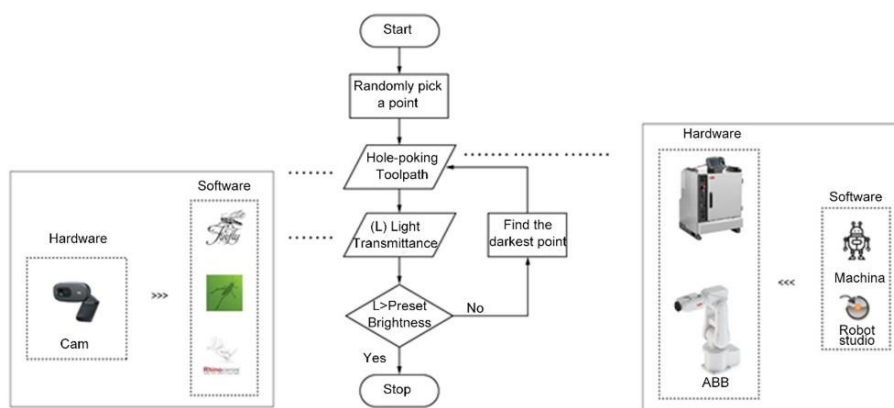


Fig.13 Real-time control process

In order to respond to the influence of solar radiation received by the building façade: since the building façade shows a high to low value of solar radiation from the upper right to the lower left, the distribution of holes follows a gradual increase from the upper right to the lower left. The trend is to add more direct light to the poorly lit areas (shown in Figure 12).

First a set of predefined hole information, including location, orientation, and angle, is generated from the interior lighting requirements during the computational design phase. In the first round of poking a hole, the system will randomly pick one from the list of predefined holes and poke a hole in the clay. Then, the robot will return to its origin point. Meanwhile, the system will acquire images from the camera and then find the darkest point and the nearest predefined hole as the next poking location. At the end of each round of hole poking, the system will check whether the light data reaches the target value for indoor lighting. If yes, the system will stop, if not, it will continue to find the darkest location and poke. (Fig.14)

The system uses computer vision technology to find the darkest location for the next poke tool path, which can create an even and consistent light on each ceramic panel.

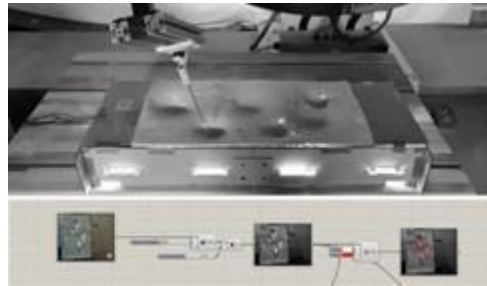


Fig.14 Real-time control computer vision and manufacturing process.

## 5 Experiment Result and Discussion

The key idea is to maximize the utilization of in-progress robotics fabrication and ceramics materiality to create a highly integrated manufacturing workflow for lighting product design and manufacture. The subsequent digital fabrication will enable the deformation and sculpting to reach all parts of complex panelized geometry and allow for the variable material thickness that can be controlled from each target point forehead. To distribute geometry variations, a computational design approach is employed within the prototype facade, and a robotic construction technique is also introduced: joining leading research in highly bespoke digital robotic fabrication. The design- research proposes handles more than just supporting bespoke transmittance outcomes; it also orchestrates custom manufacturing processes that offer designers greater material engagements, where design aspects can be positioned within material formation processes.

## 6 Future Use

The natural environment has good physiological and psychological healing effects (Zhang & Xu, 2020). At the level of physiological health, the natural environment helps to prevent chronic diseases (Knight et al., 2010) and enhance the physiological health of the group (Qin et al., 2013) at the level of psychological health, the natural environment can effectively repair attention (Bratman et al., 2015), relieve stress, and improve bad mood and mental fatigue. Especially sunlight, as an important natural factor, the strength of sunlight and the angle of sunlight are very important for treating psychological diseases and regulating the mood of users.

Therefore, creating different kinds of light can make buildings into different types of healing or immersive spaces (Figure 15, 16). In the future, it will become important to create architectural product with different light environments depending on the character of the users and the function of the space.

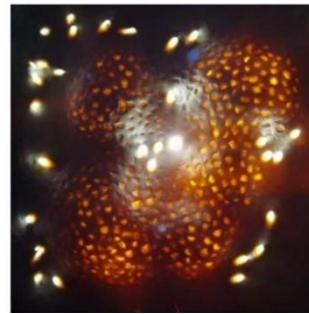
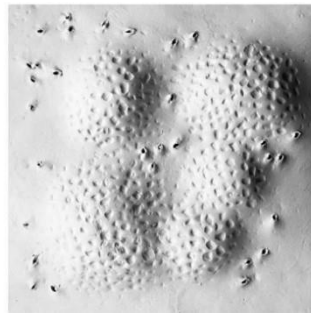


Fig.15 Ceramic prototype texture

Fig.16 Ceramic light transmittance.

## References

- Gutiérrez, R. U., & Wanner, A. (2016). Innovations in the production of ceramic luminous environments: Where craftsman meets computer. *Informes de la Construcción*, 68(544). <https://doi.org/10.3989/IC-15-167-M15>
- Ma, Z., Duenser, S., Schumacher, C., Rust, R., Bächer, M., Gramazio, F., Kohler, M., & Coros, S. (2021, August). Stylized robotic clay sculpting. *Computers & Graphics*, 98, 150–164. <https://doi.org/10.1016/j.cag.2021.05.008>
- Zhang Zhen, & Xu Lei-qing. (2020). The Healing Benefits and Application of the Virtual Natural Environment. *South Architecture*, 34–40. 10.3969/j.issn.1000-0232.2020.04.034
- Knight, T. M., Bowler, D. E., Buyung-Ali, L. M., Knight, T., & Pullin, A. S. (2010). A systematic review of evidence for the added benefits to health of exposure to natural environments. *BMC Public Health*, 10, 456. <https://doi.org/10.1186/1471-2458-10-456>

- Qin, J., Zhou, X., Sun, C., Leng, H., & Lian, Z. (2013). Influence of green spaces on environmental satisfaction and physiological status of urban residents. *Urban Forestry & Urban Greening*, 12, 490-497. <https://doi.org/10.1016/j.ufug.2013.05.005>
- Bratman, G.N., Daily, G.C., Levy, B.J., & Gross, J.J. (2015). The benefits of nature experience: Improved affect and cognition. *Landscape and Urban Planning*, 138, 41-50. <http://dx.doi.org/10.1016/j.landurbplan.2015.02.005>.